

# High-Entropy Oxides: Fundamental Aspects and Electrochemical Properties

Abhishek Sarkar, Qingsong Wang, Alexander Schiele, Mohammed Reda Chellali, Subramshu S. Bhattacharya, Di Wang, Torsten Brezesinski, Horst Hahn,\* Leonardo Velasco,\* and Ben Breitung\*

High-entropy materials, especially high-entropy alloys and oxides, have gained significant interest over the years due to their unique structural characteristics and correlated possibilities for tailoring of functional properties. The developments in the area of high-entropy oxides are highlighted here, with emphasis placed on their fundamental understanding, including entropy-dominated phase-stabilization effects and prospective applications, e.g., in the field of electrochemical energy storage. Critical comments on the different classes of high-entropy oxides are made and the underlying principles for the observed properties are summarized. The diversity of materials design, provided by the entropy-mediated phase-stabilization concept, allows engineering of new oxide candidates for practical applications, warranting further studies in this emerging field of materials science.

## 1. Introduction

One of the fundamental driving forces in materials science is the development of advanced materials with tailorable properties. A new concept of materials design, rendering the possibility to affect the phase stability of solid solutions through precise control of configurational entropy, has evolved with the discovery of high entropy alloys (HEAs).<sup>[1,2]</sup> More recently, the field of high entropy materials has been broadened to include different groups of nonmetallic compounds, like oxides,<sup>[3]</sup> carbides,<sup>[4]</sup> borides<sup>[5]</sup> nitrides,<sup>[6]</sup> and sulfides.<sup>[7]</sup> Rost et al. discovered the possibility to incorporate five different cations, in equiatomic ratios, into a single-phase oxide system and defined this as “entropy-stabilized oxide” due to the clear evidence of an entropy-driven structural stabilization effect.<sup>[3]</sup> In subsequent publications by Bérardan

et al., a more general nomenclature, “high-entropy oxides (HEOs)” analogous to “high entropy alloys,” has been established to classify multicationic equiatomic oxide systems.<sup>[8–10]</sup> The same nomenclature, HEOs, has been used here. HEOs are located at the center of a multinary phase diagram, which is often the least explored realm of materials compositions, therefore unexpected behaviors can be anticipated.<sup>[8,9,11,12]</sup> The formation of chemically complex, single-phase HEOs is noteworthy, since enthalpy-dominated phase separation is a common scenario in most of the complex multinary systems. Investigations into these new material classes have already resulted in many unexpected and inter-

esting findings. Considering the increasing attention being paid to this promising design concept of oxides, the recent results and achievements in the field of HEOs are highlighted in this research news article.

## 2. Entropy Stabilization Concept and Structural Features

### 2.1. High-Entropy Concept and Entropy-Based Material's Classification

The general concept of entropy stabilization is based on the possibility to stabilize a single-phase crystal structure by increasing the configurational entropy ( $S_{\text{config}}$ ) of the system. This can be

A. Sarkar, Dr. Q. Wang, A. Schiele, Dr. M. R. Chellali, Dr. D. Wang, Dr. T. Brezesinski, Prof. H. Hahn, Dr. L. Velasco, Dr. B. Breitung  
Institute of Nanotechnology  
Karlsruhe Institute of Technology (KIT)  
76344 Eggenstein-Leopoldshafen, Germany  
E-mail: horst.hahn@kit.edu; leonardo.estrada@kit.edu;  
ben.breitung@kit.edu

The ORCID identification number(s) for the author(s) of this article can be found under <https://doi.org/10.1002/adma.201806236>.

© 2019 The Authors. Published by WILEY-VCH Verlag GmbH & Co. KGaA, Weinheim. This is an open access article under the terms of the Creative Commons Attribution-NonCommercial-NoDerivs License, which permits use and distribution in any medium, provided the original work is properly cited, the use is non-commercial and no modifications or adaptations are made.

DOI: 10.1002/adma.201806236

A. Sarkar, Prof. H. Hahn  
Joint Research Laboratory Nanomaterials – Technische Universität  
Darmstadt and Karlsruhe Institute of Technology (KIT)  
64287 Darmstadt, Germany

Prof. S. S. Bhattacharya  
Nano Functional Material Technology Centre  
Department of Metallurgical and Materials Engineering  
Indian Institute of Technology Madras  
Chennai 600036, India

Dr. D. Wang, Dr. B. Breitung  
Karlsruhe Nano Micro Facility  
Karlsruhe Institute of Technology (KIT)  
76344 Eggenstein-Leopoldshafen, Germany

Prof. H. Hahn  
Helmholtz Institute Ulm for Electrochemical Energy Storage (HIU)  
89081 Ulm, Germany

done by increasing the number of elements, randomly distributed on the same lattice sites. The molar configurational entropy of oxide systems can be calculated according to Equation (1)<sup>[12]</sup>

$$S_{\text{config}} = -R \left[ \left( \sum_{i=1}^N x_i \ln x_i \right)_{\text{cation-site}} + \left( \sum_{j=1}^M x_j \ln x_j \right)_{\text{anion-site}} \right] \quad (1)$$

where  $x_i$  and  $x_j$  represent the mole fraction of elements present in the cation and anion sites, respectively, and  $R$  is the universal gas constant. For HEOs, the contribution of the anion site is expected to only have a minor effect on  $S_{\text{config}}$ , given that only one anion is present (i.e., the effect of possible oxygen vacancies is not considered).  $S_{\text{config}}$  in an  $N$ -components solid solution (with  $N = 2, 3, 4,$  or  $5$ ) as a function of the mole fraction of the  $N$ th component is plotted in Figure 1a.<sup>[3]</sup> It can be observed that  $S_{\text{config}}$  increases with the addition of more elements to a given system. Furthermore,  $S_{\text{config}}$  reaches a maximum when all elements are present in equiatomic fractions (Figure 1a). In an equiatomic 5-cation system, the maximum  $S_{\text{config}}$  value that can be achieved is 1.61  $R$ . As per empirical classification, based on its configurational entropy introduced by Murty et al.,<sup>[12]</sup> materials with  $S_{\text{config}} \geq 1.5 R$  can be classified as “high entropy”, materials with  $1.5 R > S_{\text{config}} \geq 1 R$  as “medium entropy” and materials with  $S_{\text{config}} < 1 R$  as “low entropy” systems. The dependency of the free energy of mixing ( $\Delta G_{\text{mix}}$ ) on the enthalpy of mixing ( $\Delta H_{\text{mix}}$ ) and the entropy of mixing ( $\Delta S_{\text{mix}}$ ) is presented in Equation (2).

$$\Delta G_{\text{mix}} = \Delta H_{\text{mix}} - T\Delta S_{\text{mix}} \quad (2)$$

In many cases, a single phase is achieved if  $S_{\text{config}} \geq 1.5 R$ , as then the  $T\Delta S_{\text{mix}}$  can be large enough to dominate the free energy landscape and overcome  $\Delta H_{\text{mix}}$ . This emphasizes the fact that high temperatures are beneficial in the formation of high or medium entropy (single-phase) systems; at room temperature, many these systems must be considered metastable. However, several studies have already shown that this criterion ( $S_{\text{config}} \geq 1.5 R$ ) does not guarantee the formation of a single-phase material.<sup>[11,12]</sup> In many cases, the configurational entropy gain is not enough to compensate for  $\Delta H_{\text{mix}}$  and, as a result, intermediate products with more favorable formation enthalpies are produced.<sup>[11,12]</sup> Still, in most of the research on multicomponent near-equiatomic systems the term “high entropy” is commonly used, as there is an assured  $S_{\text{config}}$  gain (following Boltzmann’s entropy Equation (1)) with addition of more elements.<sup>[5,6,8,9,11–14]</sup>

## 2.2. Structural Features of High-Entropy Oxides

Initial studies on HEOs concentrated on systems with a rock-salt structure, consisting of only one Wyckoff site for the cations.<sup>[3]</sup> The first investigated system of this materials class was  $(\text{Co}_{0.2}\text{Cu}_{0.2}\text{Mg}_{0.2}\text{Ni}_{0.2}\text{Zn}_{0.2})\text{O}$ <sup>[3]</sup> and, for simplicity, here it is termed rock-salt type HEO (R-HEO). X-ray diffraction (XRD) measurements on R-HEO and corresponding structural analysis confirmed the crystallization of a single-phase rock-salt structure, as shown in Figure 1b.<sup>[3,8,15]</sup> The range of HEOs has since widened to include a single-phase fluorite structure, resulting from the incorporation of five (or more) equiatomic cations, mostly rare-earth elements, here termed fluorite type

HEO (F-HEO); see Figure 1c.<sup>[16–18]</sup> However, both R-HEO and F-HEO comprise only one Wyckoff site for the cations. Thus, the formation of single-phase perovskite-based HEO (PE-HEO) and spinel-based HEO (SP-HEO) materials was important in providing evidence that this design concept can be extended to structures with multiple cation sites.<sup>[13,19–21]</sup> Figure 1d shows two single-phase orthorhombic PE-HEOs with 6 and 10 cations.<sup>[20]</sup> The 6-cation PE-HEO,  $(\text{Gd}_{0.2}\text{La}_{0.2}\text{Nd}_{0.2}\text{Sm}_{0.2}\text{Y}_{0.2})\text{MnO}_3$ , reveals the possibility to stabilize multiple A-site cations in an orthorhombic structure upon heat-treatment above 900 °C. The 10-cation PE-HEO,  $(\text{Gd}_{0.2}\text{La}_{0.2}\text{Nd}_{0.2}\text{Sm}_{0.2}\text{Y}_{0.2})(\text{Co}_{0.2}\text{Cr}_{0.2}\text{Fe}_{0.2}\text{Mn}_{0.2}\text{Ni}_{0.2})\text{O}_3$ , on the other hand, illustrates the possibility to form a chemically complex HEO, wherein both the A- and B-sites are populated by multiple cations and all the constituent elements are uniformly distributed on the respective sites.<sup>[20]</sup>

One important factor affecting the configurational entropy is the local structure of HEOs, as any type of clustering or segregation of elements will decrease the number of possible microstates, thereby lowering the overall entropy.<sup>[12]</sup> Figure 1e shows a high-resolution transmission electron microscopy (HR-TEM) image along with a selected-area electron diffraction (SAED) pattern of R-HEO.<sup>[22]</sup> The well-defined lattice fringes and the SAED results indicate the absence of local clustering (of secondary phases), in agreement with the XRD findings, confirming the phase purity of material. The corresponding elemental distribution maps obtained by scanning TEM (STEM)–energy-dispersive X-ray spectroscopy (STEM–EDX, Figure 1f) demonstrate the homogeneity of R-HEO even on the nanometer length scale.<sup>[3,22]</sup> Consistent results were obtained for other HEOs, such as F-HEO and PE-HEO.<sup>[13,16,18,20]</sup> Extended X-ray absorption fine structure (EXAFS) studies on R-HEO (Figure 1g) suggest random distribution of elements in the crystal lattice, owing to the fact that the local chemical environment for all cations is found to be nearly identical.<sup>[3,23]</sup> The combination of these results confirms the single-phase nature and the statistical distribution of cations in the specific sublattice.

## 2.3. Entropy-Dominated Phase-Stabilization Effects

The entropy-based phase-stabilization effect in HEOs is demonstrated by a set of controlled experimental results obtained from the heat-treatment of HEOs at different temperatures.<sup>[3,15,20]</sup> In many cases, like for  $(\text{Co}_{0.2}\text{Cu}_{0.2}\text{Mg}_{0.2}\text{Ni}_{0.2}\text{Zn}_{0.2})\text{O}$ ,  $(\text{Ce}_{0.2}\text{Zr}_{0.2}\text{Hf}_{0.2}\text{Sn}_{0.2}\text{Ti}_{0.2})\text{O}_2$ , or  $(\text{Gd}_{0.2}\text{La}_{0.2}\text{Nd}_{0.2}\text{Sm}_{0.2}\text{Y}_{0.2})\text{MnO}_3$ , the system undergoes a reversible phase transformation from single-phase solid solution to multiphase mixture when calcined at relatively lower temperatures.<sup>[3,8,18,20,24]</sup> For R-HEO (Figure 1h), demixing of the rock-salt structure is observed when the system is heat-treated at 750 °C.<sup>[3]</sup> The single-phase state is regained upon subsequent heating at 1000 °C. This reversible transformation supports the entropy-dominated phase-stabilization concept, as at lower temperatures the overall  $T\Delta S_{\text{mix}}$  term might not be large enough to compensate for the enthalpy-driven phase separation. Hence, systems that show this kind of behavior, e.g.,  $(\text{Co}_{0.2}\text{Cu}_{0.2}\text{Mg}_{0.2}\text{Ni}_{0.2}\text{Zn}_{0.2})\text{O}$ , can be classified as entropy-stabilized, which is an important subset of HEOs. This reversible phase transformation is further supported by the calorimetry data for

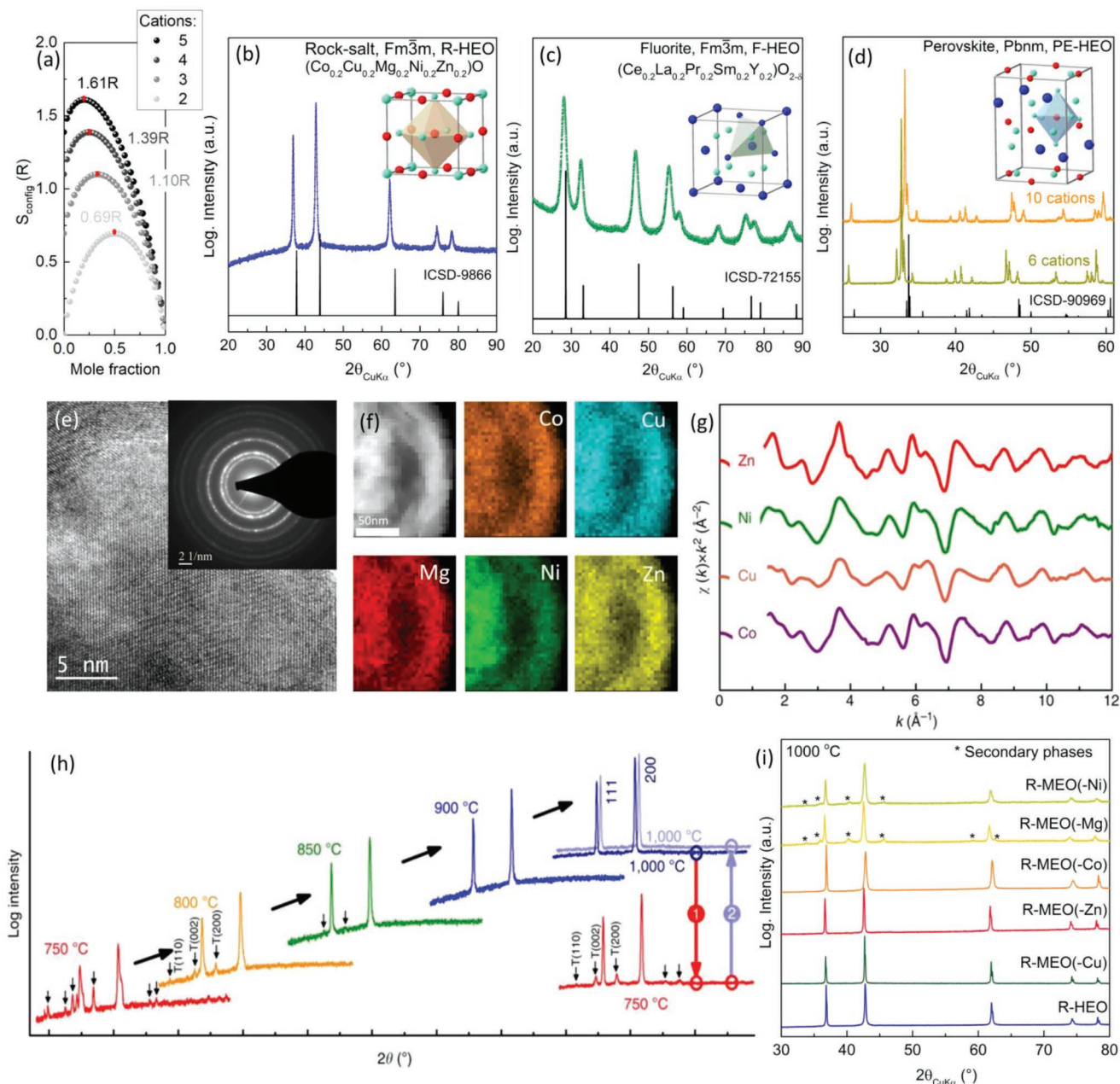


**Figure 1.** a) Dependence of configurational entropy on the number of elements. XRD patterns of HEO systems: b) R-HEO, c) F-HEO, and d) PE-HEOs. e) HR-TEM image and SAED pattern of R-HEO. f) STEM image and elemental distribution maps indicating chemical uniformity of R-HEO. g) Random distribution of cations from EXAFS. h) Reversible phase transformation as an indication of entropy stabilization effect. i) XRD patterns of different types of R-MEOs. a,g,h) Reproduced under the terms of the CC-BY 4.0 license (<http://creativecommons.org/licenses/by/4.0/>).<sup>[3]</sup> Copyright 2015, the authors, published by Springer Nature. b) Reproduced with permission.<sup>[15]</sup> Copyright 2017, Elsevier. c) Reproduced under the terms of the CC-BY 4.0 license (<http://creativecommons.org/licenses/by/4.0/>).<sup>[16]</sup> Copyright 2017, the authors, published by Taylor and Francis. d) Reproduced with permission.<sup>[20]</sup> Copyright 2018, Elsevier. e,f,i) Reproduced under the terms of the CC-BY 4.0 license (<http://creativecommons.org/licenses/by/4.0/>).<sup>[22]</sup> Copyright 2018, the authors, published by Springer Nature.

R-HEO,<sup>[3,25]</sup> which again indicate an entropy-driven structural stabilization effect, as the transformation from the multiphase (enthalpy favorable) mixture to the single-phase entropy-stabilized material is endothermic in nature.<sup>[3,25,26]</sup> This reversible phase transformation upon cyclic heat-treatment is not observed for many other classes of HEOs, for instance  $(\text{Ce}_{0.2}\text{La}_{0.2}\text{Pr}_{0.2}\text{Sm}_{0.2}\text{Y}_{0.2})\text{O}_{2-\delta}$ ,  $(\text{Gd}_{0.2}\text{La}_{0.2}\text{Nd}_{0.2}\text{Sm}_{0.2}\text{Y}_{0.2})\text{FeO}_3$ , etc.<sup>[13,16,17]</sup>

The preservation of the single-phase lattice in these cases can be attributed to the formation of a thermodynamically favorable structure, i.e.,  $\Delta H_{\text{mix}}$  is already negative. Hence,  $\Delta G_{\text{mix}}$  will be low (zero or negative) and the influence of  $T\Delta S_{\text{mix}}$  will be minimal.<sup>[20]</sup> Therefore, in **Table 1**, different kinds of HEOs reported to date are listed along with a distinction for the systems that show the entropy stabilization effect (cyclic heat-treatment behavior).

**Table 1.** List of published works on different high-entropy oxides. The table is divided into four different crystal structures along with a clear distinction between the entropy-stabilized and nonentropy-stabilized HEOs.

HEO compositions	Entropy stabilization	Literature reference
Rock-salt-type HEOs (R-HEOs)		
(Co <sub>0.2</sub> Cu <sub>0.2</sub> Mg <sub>0.2</sub> Ni <sub>0.2</sub> Zn <sub>0.2</sub> )O (Several derivatives of this system containing additional elements like Li, Na, Ga, K, etc.)	Yes	[3,8–10,15,23–25,28–30]
Fluorite-type HEOs (F-HEOs)		
(Ce <sub>0.2</sub> La <sub>0.2</sub> Sm <sub>0.2</sub> Pr <sub>0.2</sub> Y <sub>0.2</sub> )O <sub>2-δ</sub> (Nd <sub>0.16</sub> Ce <sub>0.16</sub> La <sub>0.16</sub> Sm <sub>0.16</sub> Pr <sub>0.16</sub> Y <sub>0.16</sub> )O <sub>2-δ</sub> (Hf <sub>0.2</sub> Zr <sub>0.2</sub> Ce <sub>0.2</sub> )(Y <sub>0.2</sub> Gd <sub>0.2</sub> )O <sub>2-δ</sub> (Hf <sub>0.25</sub> Zr <sub>0.25</sub> Ce <sub>0.25</sub> )(Y <sub>0.125</sub> Ca <sub>0.125</sub> )O <sub>2-δ</sub> (7 more derivatives of these systems)	No No <sup>a)</sup>	[16,31] [17]
(Ce <sub>0.2</sub> Zr <sub>0.2</sub> Hf <sub>0.2</sub> Sn <sub>0.2</sub> Ti <sub>0.2</sub> )O <sub>2</sub>	Yes	[18]
Perovskite-type HEOs (PE-HEOs)		
Ba(Zr <sub>0.2</sub> Sn <sub>0.2</sub> Ti <sub>0.2</sub> Hf <sub>0.2</sub> Nb <sub>0.2</sub> )O <sub>3</sub> Sr(Zr <sub>0.2</sub> Sn <sub>0.2</sub> Ti <sub>0.2</sub> Hf <sub>0.2</sub> Nb <sub>0.2</sub> )O <sub>3</sub> (Sr <sub>0.5</sub> Ba <sub>0.5</sub> )(Zr <sub>0.2</sub> Sn <sub>0.2</sub> Ti <sub>0.2</sub> Hf <sub>0.2</sub> Nb <sub>0.2</sub> )O <sub>3</sub> (11 more derivatives of these systems)	No <sup>a)</sup>	[13,21]
(Gd <sub>0.2</sub> La <sub>0.2</sub> Nd <sub>0.2</sub> Sm <sub>0.2</sub> Y <sub>0.2</sub> )(Co <sub>0.2</sub> Cr <sub>0.2</sub> Fe <sub>0.2</sub> Mn <sub>0.2</sub> Ni <sub>0.2</sub> )O <sub>3</sub> La(Co <sub>0.2</sub> Cr <sub>0.2</sub> Fe <sub>0.2</sub> Mn <sub>0.2</sub> Ni <sub>0.2</sub> )O <sub>3</sub> (Gd <sub>0.2</sub> La <sub>0.2</sub> Nd <sub>0.2</sub> Sm <sub>0.2</sub> Y <sub>0.2</sub> )FeO <sub>3</sub> (7 more derivatives of these systems)	No	[20]
(Gd <sub>0.2</sub> La <sub>0.2</sub> Nd <sub>0.2</sub> Sm <sub>0.2</sub> Y <sub>0.2</sub> )MnO <sub>3</sub>	Yes	[20]
Spinel-type HEOs (SP-HEOs)		
(Co <sub>0.2</sub> Cr <sub>0.2</sub> Fe <sub>0.2</sub> Mn <sub>0.2</sub> Ni <sub>0.2</sub> ) <sub>3</sub> O <sub>4</sub>	No <sup>a)</sup>	[19]

<sup>a)</sup>Cyclic heat-treatment has not been reported in the literature.

Another indication of the entropy-based phase-stabilization effect can be observed by intentionally changing the  $S_{\text{config}}$  of the systems. Lowering the  $S_{\text{config}}$  can be achieved by reducing the number of constituent cations (Equation (1)). Analogous to medium entropy alloys, four equiatomic cationic systems are classified as “medium entropy” oxides, MEOs, as the  $S_{\text{config}} = 1.39 R$ .<sup>[12,22]</sup> Rock-salt type MEOs are termed R-MEOs(-X), wherein X represents the cation removed from the parent R-HEO, i.e., (Co<sub>0.2</sub>Cu<sub>0.2</sub>Mg<sub>0.2</sub>Ni<sub>0.2</sub>Zn<sub>0.2</sub>)O. Of note, the MEO and HEO classification is only valid for isothermal material comparisons. Because the configurational entropy in MEOs is lower than in HEOs, the former often require higher synthesis temperatures than HEOs to compensate for their lower entropy to form a single phase.<sup>[3,22,27]</sup> This is illustrated in Figure 1i, in which R-MEOs(-X), synthesized at the same temperature as R-HEO, needed an additional heat-treatment step at 1000 °C to form single-phase compounds. In some cases, like R-MEO(-Ni) or R-MEO(-Mg), single-phase materials cannot be obtained, even after treatment at 1000 °C, as in these cases the  $\Delta H_{\text{mix}}$  term may be significantly larger.<sup>[3,22]</sup> These experimental observations provide clear indications of an  $S_{\text{config}}$ -based phase-stabilization effect in R-HEOs and have been recently supported by theoretical (molecular dynamics) studies by Anand et al.<sup>[27]</sup>

### 3. Electrochemical Properties

Apart from the structural features, the driving factors for the increasing interest in HEOs are their tailorable properties, which can be utilized in many different areas of application.<sup>[8,28–31]</sup> Chen et al. showed that R-HEO can act as a CO

oxidation catalyst and as a support to stabilize single atomically dispersed platinum species.<sup>[28]</sup> More recently, there have been reports regarding the thermal properties of HEOs, where an interesting correlation between the low thermal conductivity and the disorder in the systems (i.e., multiple cations acting as phonon scatters) has been observed.<sup>[17,30]</sup> Reports are also available on thin film deposition,<sup>[21,32]</sup> sintering,<sup>[24,25,29]</sup> mechanical,<sup>[17,29]</sup> magnetic,<sup>[33]</sup> and optical properties<sup>[31]</sup> of HEOs. Theoretical studies have not been extensively performed on all classes of HEOs, nevertheless, there are reports on R-HEO, which correlate: (i) the lattice distortion with the Jahn–Teller effect and (ii) the phase composition with the thermodynamic parameters.<sup>[27,34,35]</sup> The main focus of this research news article is on the electrochemical energy storage properties of R-HEOs, which will be discussed in detail below.

Bérardan et al. reported that R-HEOs exhibit colossal dielectric constants, which can further be tailored by changing the fraction of constituent elements.<sup>[8,10]</sup> This study, along with the work done on high-entropy nitrides for supercapacitors,<sup>[6]</sup> indicates that high-entropy materials are interesting for applications in modern microelectronics and for the development of new capacitance-based energy storage devices. The same group showed that a large fraction of aliovalent dopants (Li<sup>+</sup>, Na<sup>+</sup>, K<sup>+</sup>, etc.) can be incorporated into a single-phase R-HEO lattice due to two reasons: (i) Internal defect formation (e.g., oxygen vacancies) and (ii) internal charge compensation within the system, which is achieved by oxidation of Co<sup>2+</sup> to Co<sup>3+</sup>. Doped R-HEOs, especially those containing alkali ions (Li<sup>+</sup> or Na<sup>+</sup>), revealed interesting transport properties. It was found that at room temperature the Li-ion conductivity of Li-doped R-HEO was on the order of 10<sup>-3</sup> S cm<sup>-1</sup>.<sup>[9]</sup> Furthermore, it increased with doping

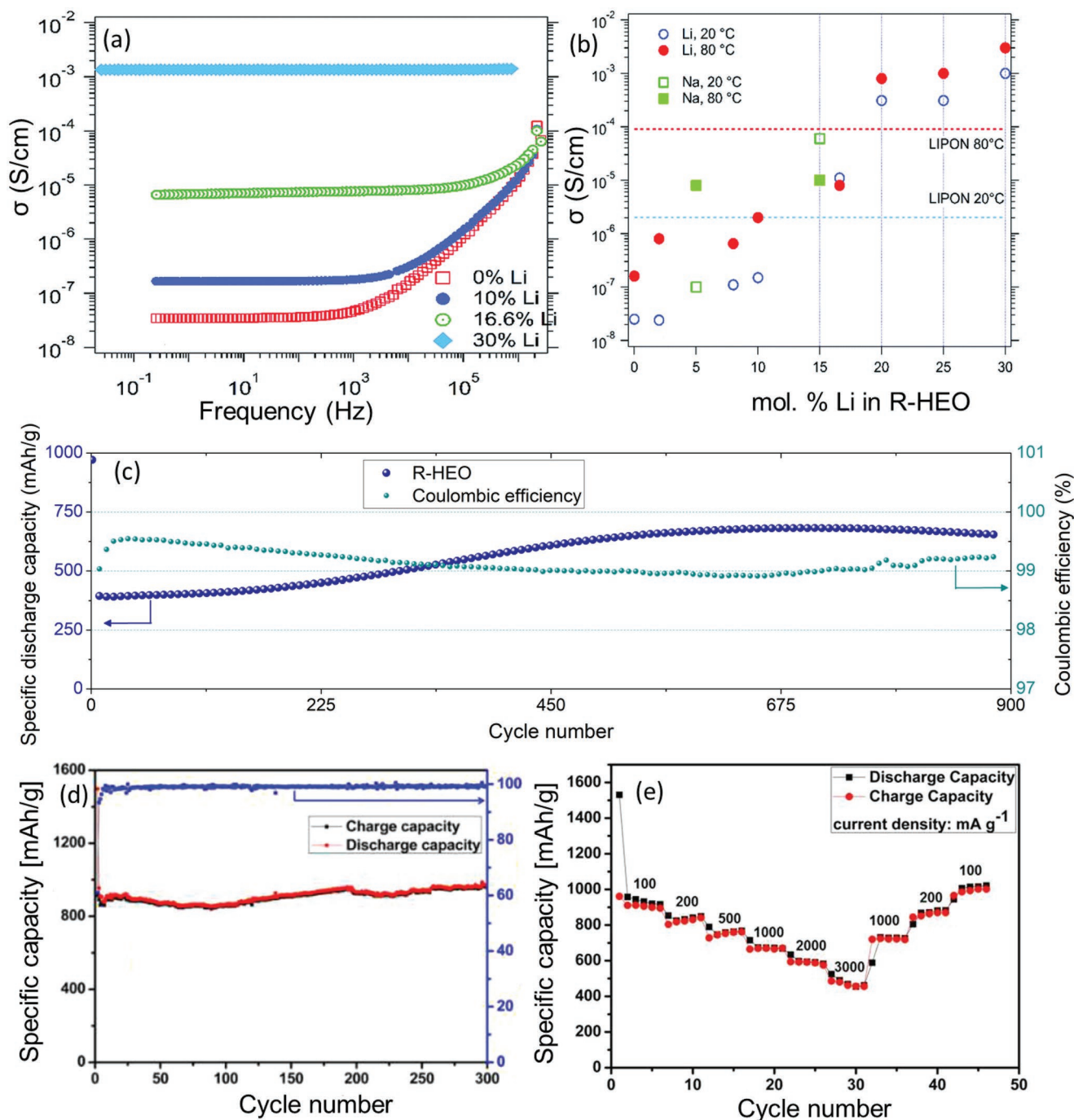


**Figure 2.** a) Variation in ionic conductivity with Li<sup>+</sup>-doping level in R-HEO. b) Comparison of ionic conductivities of Li<sup>+</sup>- and Na<sup>+</sup>-doped R-HEOs. c) Long-term cycling performance and Coulombic efficiency of R-HEO cells at 200 mA g<sup>-1</sup> using micrometer-sized particles. d) Long-term cycling performance and Coulombic efficiency of R-HEO with nanometer-sized particles. e) Rate performance test of nanometer-sized R-HEO with the specific current given in units of mA g<sup>-1</sup>. a,b) Reproduced with permission.<sup>[9]</sup> Copyright 2016, Royal Society of Chemistry. c) Reproduced under the terms of the CC-BY 4.0 license (<http://creativecommons.org/licenses/by/4.0/>).<sup>[22]</sup> Copyright 2018, the authors, published by Springer Nature. d,e) Reproduced with permission.<sup>[40]</sup> Copyright 2018, Elsevier.

level, from 10<sup>-8</sup> S cm<sup>-1</sup> (pristine R-HEO) to 10<sup>-3</sup> S cm<sup>-1</sup> (30% Li-doped), as displayed in **Figure 2a**. These results indicate the large domain of composition-based tailorable properties in HEOs. Na-ion conductivities, on the order of 10<sup>-6</sup> S cm<sup>-1</sup>, have also been reported for this material class.<sup>[9]</sup> These ionic mobility

values are rather high, especially when compared to many of the existing solid-state electrolytes (Figure 2b), and therefore, HEOs might show promise for use in all-solid-state battery cells.<sup>[36–39]</sup> From a series of controlled experiments, it has been deduced that alkali ions (Li<sup>+</sup> and Na<sup>+</sup>) likely move through the

oxygen vacancies that are created in the R-HEO lattice upon their incorporation.<sup>[9]</sup> These ionic conductivities are also much larger than the electronic one ( $\approx 10^{-9}$  S cm<sup>-1</sup>), opening up the possibility to use R-HEOs as pure ionic conductors, as the leakage current will be negligible.

The aforementioned results on the Li-ion conductivity of R-HEOs motivated subsequent studies regarding their performance in Li-ion battery cells.<sup>[22,40]</sup> It can be seen that the R-HEO shows promising long-term cycling stability (over 900 cycles), with specific capacities  $>650$  mAh g<sup>-1</sup> and Coulombic efficiencies  $>99.5\%$  at a specific current of 200 mA g<sup>-1</sup> (Figure 2c)<sup>[22]</sup> despite the use of micrometer-sized particles. Moreover, Qiu et al. reported an increase in specific capacity to  $>900$  mAh g<sup>-1</sup> for more than 300 cycles (Figure 2d) when using R-HEO with nanometer-sized particles.<sup>[40]</sup> R-HEO with micrometer-sized particles revealed a rate capability behavior with complete capacity recovery, even after cycling at high specific currents.<sup>[22]</sup> Qiu et al. showed that decreasing the particle size clearly improves the rate performance (Figure 2e); the cells delivered large specific capacities of about 490 mAh g<sup>-1</sup> at a specific current of 3000 mA g<sup>-1</sup>, with capacity recovery to  $\approx 1000$  mAh g<sup>-1</sup> at 100 mA g<sup>-1</sup>.<sup>[40]</sup> These results demonstrate that even higher specific capacities can be achieved upon further optimization in terms of particle size, electrolyte, binder, etc. The voltage profiles of R-HEO are indicative of a conversion type reaction, with virtually linear voltage decay over the entire potential range after the first cycle.<sup>[22,40]</sup>

As mentioned in the previous section, an entropy-mediated phase-stabilization effect is known for R-HEOs.<sup>[3]</sup> A profound effect of entropy on the electrochemical characteristics of R-HEO has been observed, too.<sup>[22]</sup> By extracting one of the present cations from the R-HEO the entropy decreases from 1.61 R to 1.39 R, as explained in Section 2.3., and the electrochemical characteristics are significantly altered (Figure 3). Evidently, the R-HEO exhibits much improved capacity retention over the first 100 cycles compared to the R-MEO(-X) compounds, thus indicating that the transition to medium entropy compounds results in significant performance decay (Figure 3a). This finding leads us to the conclusion that entropy stabilization possibly plays an important role in achieving a stable conversion reaction mechanism.<sup>[22]</sup> The Coulombic

efficiencies corroborate this interpretation by showing the highest values for R-HEO.<sup>[22]</sup> A complete cell failure within approximately ten cycles is observed for R-MEO(-Co), indicating the importance of Co in the system (Figure 3a). The significance of certain elements, like Co and Mg, to achieve stable cycling performance has also been observed by Qiu et al.<sup>[40]</sup> The extraction of constituent cations leads to completely different effects on the electrochemical behavior. For example, a much lower lithiation potential is found when Cu is removed from the R-HEO (Figure 3b), while a two-step oxidation with delithiation is seen when Zn is absent.<sup>[22]</sup> Such element specific behavior may help to design or tailor electrode materials to specific user needs.

The stable cycling behavior of R-HEO observed for both micrometer- and nanometer-sized particles is in fact interesting. During the course of the initial lithiation, the XRD reflections of R-HEO vanished (Figure 4a), thus indicating an X-ray amorphous structure after the first half-cycle. However, no other reflections (from secondary phases) or reappearance of the initial reflections, even after subsequent delithiation, were observed. This behavior is typical of conversion electrode materials and can be explained by formation of very small and highly defective crystallites, whose sizes are often below the coherence length of X-rays. Using SAED, a rock-salt structure was clearly identified, even at the fully lithiated state, where only Li<sub>2</sub>O and corresponding metals should be present (Figure 4a). Upon subsequent delithiation the rock-salt structure could still be observed.<sup>[22]</sup> The corresponding STEM-EDX elemental distribution maps demonstrate the homogeneity (no element segregation) of R-HEO after one complete cycle (Figure 4b). This in turn demonstrates the possibility of preserving a stable R-HEO host matrix during the entire conversion process, facilitating reintegration of metal cations in the delithiation cycle.<sup>[22]</sup> Additionally, SAED rings after the first lithiation indicate the presence of Li<sub>2</sub>O, thereby supporting the assumption of a conversion-based reaction during cycling operation (Figure 4c). The host rock-salt structure of R-HEO can still be identified after ten cycles from the SAED pattern shown in Figure 4d. The as-synthesized R-HEO (Figure 1e) shows a well-defined lattice, while a defective structure is evident after ten cycles (indicated by red circles in Figure 4e). Consequently, an entropy-stabilized

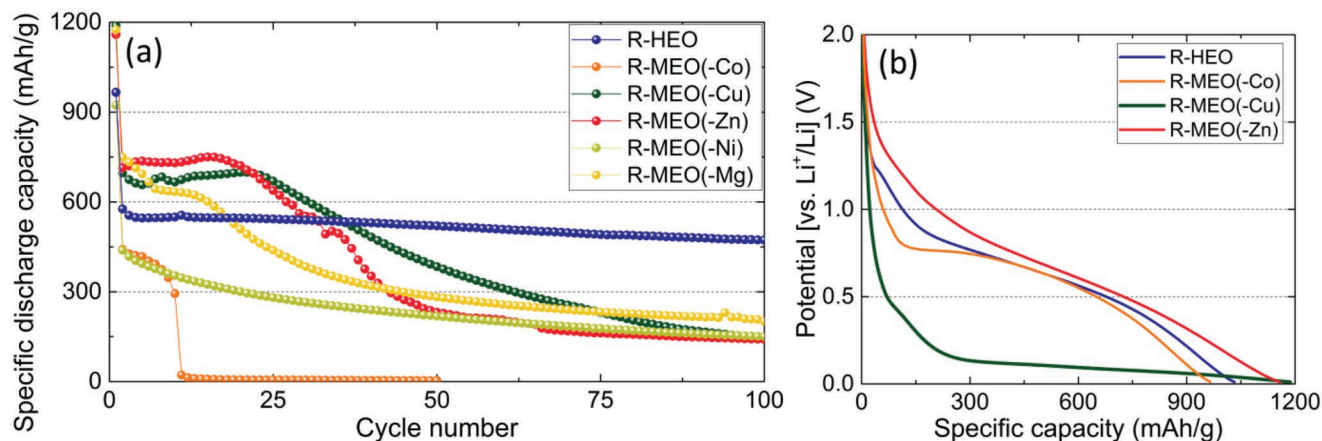


**Figure 3.** a) Specific capacity over 100 cycles and b) the first lithiation profiles of different compounds. a,b) Reproduced under the terms of the CC-BY 4.0 license (<http://creativecommons.org/licenses/by/4.0/>).<sup>[22]</sup> Copyright 2018, the authors, published by Springer Nature.

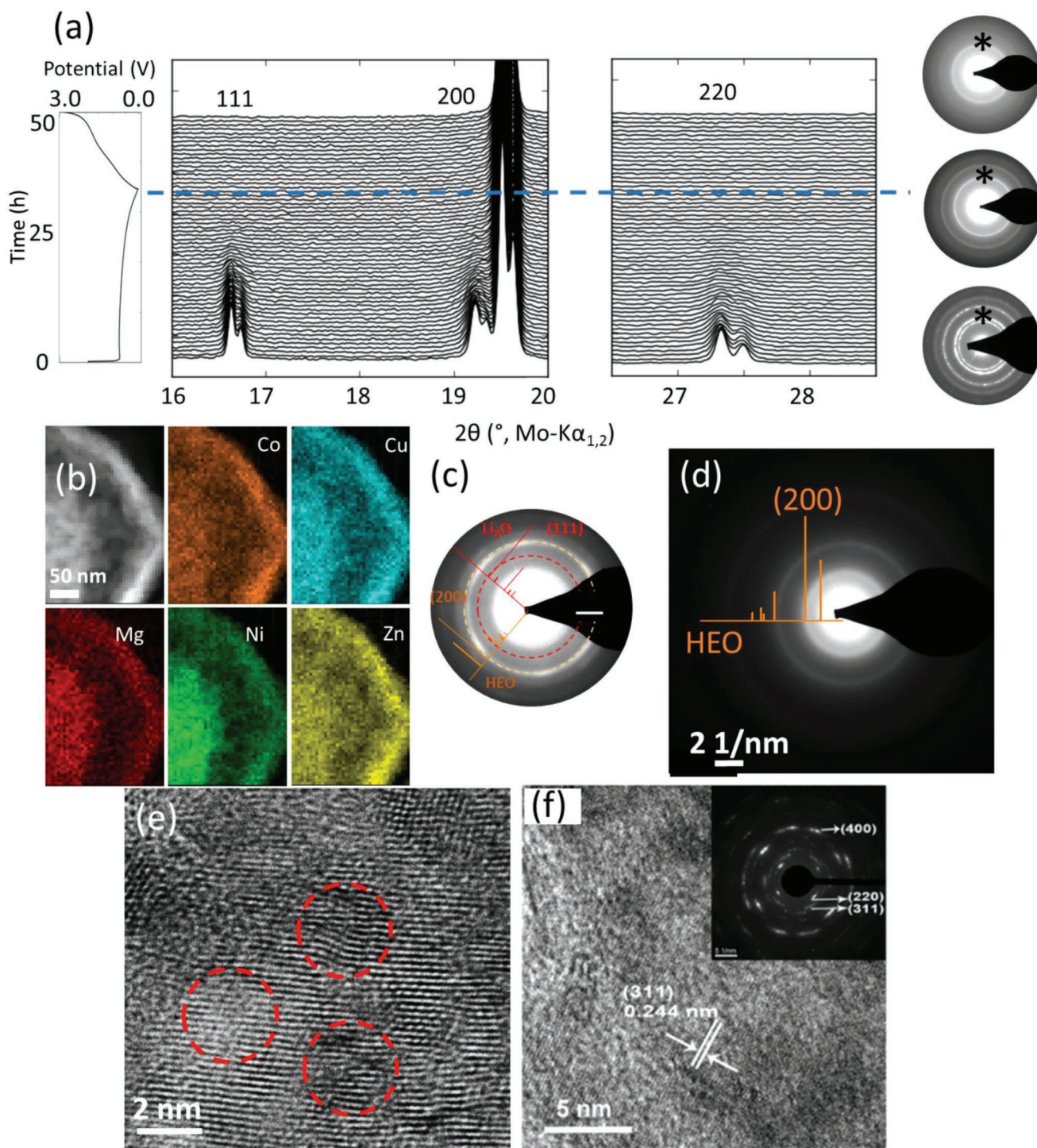


**Figure 4.** a) Operando XRD and SAED patterns. b) The uniform elemental distribution is evidenced by STEM–EDX. c) Formation of  $\text{Li}_2\text{O}$  visualized by SAED. d,e) Preserved rock-salt structure of R-HEO after ten cycles. f) Rock-salt structure in nanometer-sized R-HEO after 300 cycles. a–e) Reproduced under the terms of the CC-BY 4.0 license (<http://creativecommons.org/licenses/by/4.0/>).<sup>[22]</sup> Copyright 2018, the authors, published by Springer Nature. f) Reproduced with permission.<sup>[40]</sup> Copyright 2018, Elsevier.

conversion reaction is hypothesized,<sup>[22]</sup> wherein a host rock-salt structure is preserved by some of the constituent elements (e.g., Mg, which does not react in the given potential range) while the others participate in the redox reactions. In the case

reported by Qiu et al., similar observations were made.<sup>[40]</sup> The SAED pattern in the inset of Figure 4f shows that the R-HEO undergoes crystallinity deterioration upon cycling, but small crystalline domains can still be identified after 300 cycles.<sup>[40]</sup>

The formation of secondary phases (metal or metal oxides) was not observed in both studies. The presence of a “stable” host lattice (probably inactive MgO) and sluggish diffusion effects were assumed by Qiu et al. to be the reasons for the structural integrity and the stable cycling performance.<sup>[40]</sup> Hence, both studies independently point toward a very similar reaction mechanism, where some of the constituent elements preserve the host lattice structure, while the others react to contribute to the capacity. Combining both mechanistic hypotheses,<sup>[22,40]</sup> it seems that the retention of R-HEO structure is possibly due to sluggish diffusion, preventing element segregation and formation of individual (binary) oxides.

#### 4. Summary and Outlook

In recent years, HEOs have evolved into a new research field. The possibility of incorporating multiple cations (five or more) into a specific lattice structure opens up new ways for designing/tailoring oxide materials. The uniform distribution of cations in HEOs, among others, strengthens the hypothesis of entropy-dominated phase-stabilization effects in these chemically complex systems. Furthermore, the unique chemistry of HEOs leads to materials with exciting and unexpected properties. The multifunctional behavior of HEO is clearly evident from the fact that there are several different properties reported (dielectric, magnetic, thermal, catalytic, etc.) for a single composition of  $(\text{Co}_{0.2}\text{Cu}_{0.2}\text{Mg}_{0.2}\text{Ni}_{0.2}\text{Zn}_{0.2})\text{O}$ . The high Li-ion conductivities along with promising Li-storage capabilities make the rock-salt-based HEOs (R-HEOs) interesting for battery applications. It has been found that the entropy stabilization not only affects the phase stability, but also the functional properties (e.g., R-HEOs exhibit much more stable and reversible de/lithiation behavior than medium entropy oxides). The combination of high Li-ion conductivities in Li-doped R-HEO with high specific capacities observed when R-HEOs are used as an electrode (anode) material indicates the possibility of fabricating all HEO-based solid-state batteries (depending upon the possibility of designing a suitable HEO-type cathode material). Overall, the HEO concept could possibly pave the way to develop advanced oxide materials, which make use of the  $S_{\text{config}}$  structure stabilization effect to advance in the areas of thermo/mechanical engineering and semi-/superconductors, to name a few. A combination of experiments and theoretical calculations is essential for this new class of oxide systems to find the right composition regime for achieving targeted functional properties.

#### Acknowledgements

The authors acknowledge financial support from the Helmholtz Association and the Deutsche Forschungsgemeinschaft (HA 1344/43-1). A.S., Q.W., B.B., and H.H. appreciate the support of EnABLES, a project funded by the European Union's Horizon 2020 research and innovation program under grant agreement no. 730957.

#### Conflict of Interest

The authors declare no conflict of interest.

#### Keywords

electrochemical energy storage, fluorite, high-entropy oxides, perovskite, rock-salt

Received: September 26, 2018

Revised: February 6, 2019

Published online:

- [1] B. Cantor, I. T. H. Chang, P. Knight, A. J. B. Vincent, *Mater. Sci. Eng. A* **2004**, 375–377, 213.
- [2] J.-W. Yeh, S.-K. Chen, S.-J. Lin, J.-Y. Gan, T.-S. Chin, T.-T. Shun, C.-H. Tsau, S.-Y. Chang, *Adv. Eng. Mater.* **2004**, 6, 299.
- [3] C. M. Rost, E. Sachet, T. Borman, A. Mobbalegh, E. C. Dickey, D. Hou, J. L. Jones, S. Curtarolo, J.-P. Maria, *Nat. Commun.* **2015**, 6, 8485.
- [4] E. Castle, T. Csanadi, S. Grasso, J. Dusza, M. Reece, *Sci. Rep.* **2018**, 8, 8609.
- [5] J. Gild, Y. Zhang, T. Harrington, S. Jiang, T. Hu, M. C. Quinn, W. M. Mellor, N. Zhou, K. Vecchio, J. Luo, *Sci. Rep.* **2016**, 6, 37946.
- [6] T. Jin, X. Sang, R. R. Unocic, R. T. Kinch, X. Liu, J. Hu, H. Liu, S. Dai, *Adv. Mater.* **2018**, 30, 1707512.
- [7] R.-Z. Zhang, F. Gucci, H. Zhu, K. Chen, M. J. Reece, *Inorg. Chem.* **2018**, 57, 13027.
- [8] D. Bérardan, S. Franger, D. Dragoe, A. K. Meena, N. Dragoe, *Phys. Status Solidi RRL* **2016**, 10, 328.
- [9] D. Bérardan, S. Franger, A. K. Meena, N. Dragoe, *J. Mater. Chem. A* **2016**, 4, 9536.
- [10] D. Bérardan, A. K. Meena, S. Franger, C. Herrero, N. Dragoe, *J. Alloys Compd.* **2017**, 704, 693.
- [11] D. B. Miracle, O. N. Senkov, *Acta Mater.* **2017**, 122, 448.
- [12] B. S. Murty, J. W. Yeh, S. Ranganathan, *High-Entropy Alloys*, Butterworth-Heinemann, London **2014**.
- [13] S. Jiang, T. Hu, J. Gild, N. Zhou, J. Nie, M. Qin, T. Harrington, K. Vecchio, J. Luo, *Scr. Mater.* **2018**, 142, 116.
- [14] J. Zhou, J. Zhang, F. Zhang, B. Niu, L. Lei, W. Wang, *Ceram. Int.* **2018**, 44, 22014.
- [15] A. Sarkar, R. Djenadic, N. J. Usharani, K. P. Sanghvi, V. S. K. Chakravadhanula, A. S. Gandhi, H. Hahn, S. S. Bhattacharya, *J. Eur. Ceram. Soc.* **2017**, 37, 747.
- [16] R. Djenadic, A. Sarkar, O. Clemens, C. Loho, M. Botros, V. S. K. Chakravadhanula, C. Kübel, S. S. Bhattacharya, A. S. Gandhi, H. Hahn, *Mater. Res. Lett.* **2017**, 5, 102.
- [17] J. Gild, M. Samiee, J. L. Braun, T. Harrington, H. Vega, P. E. Hopkins, K. Vecchio, J. Luo, *J. Eur. Ceram. Soc.* **2018**, 38, 3578.
- [18] K. Chen, X. Pei, L. Tang, H. Cheng, Z. Li, C. Li, X. Zhang, L. An, *J. Eur. Ceram. Soc.* **2018**, 38, 4161.
- [19] J. Dąbrowa, M. Stygar, A. Mikołaj, A. Knapik, K. Mroczka, W. Tejchman, M. Danielewski, M. Martin, *Mater. Lett.* **2018**, 216, 32.
- [20] A. Sarkar, R. Djenadic, D. Wang, C. Hein, R. Kautenburger, O. Clemens, H. Hahn, *J. Eur. Ceram. Soc.* **2018**, 38, 2318.
- [21] Y. Sharma, B. L. Musico, X. Gao, C. Hua, A. F. May, A. Herklotz, A. Rastogi, D. Mandrus, J. Yan, H. N. Lee, M. F. Chisholm, V. Keppens, T. Z. Ward, *Phys. Rev. Mater.* **2018**, 2, 060404.
- [22] A. Sarkar, L. Velasco, D. Wang, Q. Wang, G. Talasila, L. de Biasi, C. Kübel, T. Brezesinski, S. S. Bhattacharya, H. Hahn, B. Breitung, *Nat. Commun.* **2018**, 9, 3400.
- [23] C. M. Rost, Z. Rak, D. W. Brenner, J.-P. Maria, *J. Am. Ceram. Soc.* **2017**, 100, 2732.
- [24] A. D. Dupuy, X. Wang, J. M. Schoenung, *Mater. Res. Lett.* **2019**, 7, 60.
- [25] M. Biesuz, L. Spiridigliozzi, G. Dell'Agli, M. Bortolotti, V. M. Sglavo, *J. Mater. Sci.* **2018**, 53, 8074.



- [26] E. J. Williams, *Proc. R. Soc. London, Ser. A* **1935**, 152, 231.
- [27] G. Anand, A. P. Wynn, C. M. Handley, C. L. Freeman, *Acta Mater.* **2018**, 146, 119.
- [28] H. Chen, J. Fu, P. Zhang, H. Peng, C. W. Abney, K. Jie, X. Liu, M. Chi, S. Dai, *J. Mater. Chem. A* **2018**, 6, 11129.
- [29] W. Hong, F. Chen, Q. Shen, Y.-H. Han, W. G. Fahrenholtz, L. Zhang, *J. Am. Ceram. Soc.* **2019**, 102, 2228.
- [30] J. L. Braun, C. M. Rost, M. Lim, A. Giri, D. H. Olson, G. N. Kotsonis, G. Stan, D. W. Brenner, J.-P. Maria, P. E. Hopkins, *Adv. Mater.* **2018**, 30, 1805004.
- [31] A. Sarkar, C. Loho, L. Velasco, T. Thomas, S. S. Bhattacharya, H. Hahn, R. Djenadic, *Dalton Trans.* **2017**, 46, 12167.
- [32] G. N. Kotsonis, C. M. Rost, D. T. Harris, J.-P. Maria, *MRS Commun.* **2018**, 8, 1371.
- [33] P. B. Meisenheimer, T. J. Kratochl, J. T. Heron, *Sci. Rep.* **2017**, 7, 3.
- [34] Z. Rak, C. M. Rost, M. Lim, P. Sarker, C. Toher, S. Curtarolo, J. P. Maria, D. W. Brenner, *J. Appl. Phys.* **2016**, 120, 095105.
- [35] Z. Rák, J.-P. Maria, D. W. Brenner, *Mater. Lett.* **2018**, 217, 300.
- [36] Q. Wang, Z. Wen, J. Jin, J. Guo, X. Huang, J. Yang, C. Chen, *Chem. Commun.* **2016**, 52, 1637.
- [37] Z. Gao, H. Sun, L. Fu, F. Ye, Y. Zhang, W. Luo, Y. Huang, *Adv. Mater.* **2018**, 30, 1705702.
- [38] Z. Zhang, Y. Shao, B. Lotsch, Y. Hu, L. F. Nazar, C. Nan, J. Maier, M. Armand, L. Chen, *Energy Environ. Sci.* **2018**, 11, 1945.
- [39] F. Strauss, T. Bartsch, L. de Biasi, A.-Y. Kim, J. Janek, P. Hartmann, T. Brezesinski, *ACS Energy Lett.* **2018**, 3, 992.
- [40] N. Qiu, H. Chen, Z. Yang, S. Sun, Y. Wang, Y. Cui, *J. Alloys Compd.* **2019**, 777, 767.